Published in final edited form as:
*Mol Cancer Ther*. 2008 August ; 7(8): 2566–2573. doi:10.1158/1535-7163.MCT-08-0435.

# Relaxin Treatment of Solid Tumors – Effects on Electric Field-Mediated Gene Delivery[1]

**Joshua Henshaw**, **Brian Mossop**, and **Fan Yuan**[2]
*Department of Biomedical Engineering, Duke University, Durham, NC 27708, USA*

## Abstract

Pulsed electric fields have been shown to enhance interstitial transport of plasmid DNA pDNA in solid tumors *in vivo*. However, the extent of enhancement is still limited, partly due to the collagen component in extracellular matrix. To this end, effects of collagen remodeling on interstitial electrophoresis were investigated by pre-treatment of tumor bearing mice with a recombinant human relaxin (rh-Rlx). In the study, two tumor lines (4T1 and B16.F10) were examined; and they were implanted subcutaneously to establish two murine models: dorsal skin-fold chamber (DSC) and hind leg. Effects of rh-Rlx on pDNA electrophoresis were measured either directly in the DSC model, or indirectly in the hind leg model via reporter gene expression. It was observed that rh-Rlx treatment reduced collagen levels in the hind leg tumors but not in the DSC tumors. The observation correlated with the results from electromobility experiments, where rh-Rlx treatment enhanced transgene expression in 4T1 hind leg tumors but did not increase the electromobility of pDNA in the DSC tumors. In addition, it was observed that pDNA binding to collagen could block its diffusion in collagen gel *in vitro.* These observations demonstrated that effects of rh-Rlx on the collagen content depended on microenvironment in solid tumors and that rh-Rlx treatment would enhance electric field-mediated gene delivery only if it could effectively reduce the collagen content in collagen-rich tumors.

### Keywords

Electric field-mediated gene delivery; in vivo electrophoresis; interstitial transport; relaxin; non-viral gene delivery

## INTRODUCTION

Electric field-mediated gene delivery is a physical method for improving both *in vitro* and *in vivo* transfection efficiency with naked plasmid DNA (pDNA). Exposure to pulsed electric field has been shown to improve gene delivery in a variety of tissues, including those in solid tumors. A summary of the literature reports on electric field-mediated gene delivery in solid tumors has been provided in a recent review by Heller *et al.* (1). The majority of these reports have been focused on effects of parameters of the applied electric field (*e.g.*, electric pulse strength, duration, and number) on quantifiable outputs such as transfection efficiency (*e.g.*, reporter gene expression) or therapeutic response (*e.g.*, tumor regression). As such, mechanisms behind the improved delivery remain largely unknown. In general, electric field-

[1]This work was supported by a grant from the National Institutes of Health (CA94019)

2Request for reprints: Dr. Fan Yuan, Department of Biomedical Engineering, Duke University, 136 Hudson Hall, Durham, NC, 27708, 919-660-5411 (phone), 919-684-4488 (fax), fyuan@duke.edu (email).

mediated gene delivery involves electropermeabilization of cell membrane and electrophoresis of pDNA (1–3).

Electropermeabilization refers to the increased permeability of cell membrane to traditionally non-permeant molecules in the presence of an external electric field. This phenomenon has been studied extensively *in vitro* (4–6) and *in vivo* (7–11), and is the subject of many reviews (12–16). Electrophoresis occurs due to the polyanionic nature of pDNA under physiological conditions, which results in a force vector on the molecule in the direction of external field. The potential significance of *in vivo* electrophoresis on improved transgene expression has been demonstrated by a series of studies conducted in muscle (17,18). These studies suggested that following an initial electropermeabilizing pulse, the electrophoretic component of a pulse sequence plays an important role in improved transgene expression. The magnitude of *in vivo* electrophoretic transport in tumor interstitium has been measured both *ex vivo* (19), and *in vivo* (2). These studies concluded that a pulsed electric field was able to increase pDNA mobility, but the overall magnitude of movement with a 10-pulse sequence was less than the radius of a typical tumor cell (5 μm). The limited improvement in pDNA mobility was attributed to physiological barriers in solid tumors; and the major barrier is formed by interstitial structures.

Interstitial resistance to water and small solute transport is largely determined by hydrophilic glycosaminoglycans (GAGs) (20). However, it has been shown repeatedly that GAG content alone is not the only determinant responsible for the high transport resistance in many soft tissues (21). Solid tumors may possess unique extracellular matrix (ECM) compositions and assemblies that are substantially different from those in normal tissues (22). The differences may arise from the embryonic-like stage of development of many tumors, with extensive ECM synthesis (23). Recent studies have shown that both the content and structure of collagen, but not GAGs, are the key factors effecting macromolecular transport in tumor interstitium (24–26). This finding is supported by the *in vitro* (19) and *in vivo* (2) studies mentioned above, which show that pDNA electrophoresis correlates with tumor collagen content.

The collagen content can be altered *in vivo* through either treatment with collagenase or induction of collagen remodeling; and the latter is relatively safer compared to the former for improving gene delivery in solid tumors. The remodeling can be induced by relaxin, a 60-kDa peptide hormone belonging to the insulin family. It is a pleiotropic hormone with a wide range of biological activities including the induction of collagen remodeling in tissues of the birth canal prior to delivery (27). In addition to collagen, relaxin has also been shown to influence other molecules of the ECM, including GAGs (28) and laminin (29). A recombinant human relaxin (rh-Rlx) is available for clinical experimentation, and has gained attention for its potential therapeutic capability in the treatment of renal (30) and pulmonary fibrosis (31). Mechanisms behind relaxin's effects on collagen metabolism remain unclear; and conflicting results have been shown in similar studies on human fibroblasts where relaxin can either promote collagen synthesis in some cases (32), or decrease collagen synthesis and increase collagenase synthesis in other cases (33). The conflicting nature of these findings raises the possibility that relaxin acts through the interplay between collagen synthesis and collagen degradation (27).

Brown *et al.* have shown that chronic relaxin treatment could significantly increase diffusive transport of IgG and a dextran molecule with molecular weight of 2,000,000 (dextran 2M) in solid tumors, while the overall collagen levels remained constant (34). The increase in diffusion was attributed to a dynamic balance between the rates of up-regulations of collagen production and degradation, which maintained a steady state level of collagen but created a more porous ECM structure that was less hindrance to diffusion. In a recent study, Kim *et al.* showed that an oncolytic adenovirus, which carried the relaxin gene, exhibited greater transduction

efficiency and spatial distribution in tumors (35). The collagen content of tumors infected with the adenovirus was substantially decreased, implying that the increased virus distribution and penetration correlated with decreased collagen levels (35).

In this study, we attempted to improve the limited interstitial transport of pDNA induced by pulsed electric fields by remodeling collagen fiber matrix with chronic relaxin treatment. Changes in the collagen content were quantified in two tumor models: dorsal skin-fold chamber (DSC) and hind leg. Effects of relaxin treatment on interstitial transport were determined either directly in the DSC tumors, or indirectly in the hind leg tumors by quantifying transgene expression. In addition, a pDNA-collagen binding assay was performed to explore potential mechanisms behind the correlation between tumor collagen content and pDNA electromobility.

## MATERIALS AND METHODS

### Hind Leg Tumor Model

4T1 (a murine mammary carcinoma) and B16.F10 (a metastatic subline of B16 murine melanoma) cells were cultured in DMEM supplemented with 10 % fetal bovine serum, 100 U/ml streptomycin, and 100 U/ml penicillin at 37°C, 95 % air and 5 % carbon dioxide. Cells were harvested from flasks with 0.25 % trypsin/EDTA and rinsed with DMEM then PBS. Cells were centrifuged for 2 min at 176 g and re-suspended in PBS to a final concentration of $2 \times 10^7$ cells/ml. Female Balb/C and C57BL/6 mice (18–22 g, Charles River, Raleigh, NC) were used as hosts for 4T1 and B16.F10 tumors respectively. Mice were anesthetized with an i.p. injection of 80 mg ketamine and 10 mg xylazine per kg body weight. Hair was removed from the left and right hind legs and 50 μl of cell suspension (~$1 \times 10^6$ cells) were injected subcutaneously on the quadriceps of each leg. Tumors were allowed to grow until they reached 8–10 mm in diameter.

### Dorsal Skin-Fold Tumor Model

Dorsal skin-fold chamber tumor models were used to quantify the extent of *in vivo* electrophoresis in untreated and relaxin treated mice. 4T1 and B16.F10 cells were cultured and harvested as described previously and re-suspended to a final concentration of $5 \times 10^7$ cells/ml. Fluorescently labeled, electrically neutral, yellow-green latex microspheres with a diameter of 1.0 μm (YG-MS, Polysciences, Inc., Warrington, PA) were added to the cell suspension to be used as a tissue marker during image analysis. Female Balb/C and C57BL/6 mice (22–25 g, Charles River, Raleigh, NC) were used as hosts for 4T1 and B16.F10 tumors, respectively. DSCs were implanted in mice anesthetized with an i.p. injection of 80 mg ketamine and 10 mg xylazine per kg body weight. 10 μl of cell suspension (~$5 \times 10^5$ cells) was injected into the fascia layer at the center of the DSC, and then the DSC was sealed with a glass coverslip. Tumors were allowed to grow 5–6 days and 7–10 days for 4T1 and B16.F10, respectively.

### Relaxin Treatment

Recombinant human relaxin H2 (rh-Rlx, BAS Medical, San Mateo, CA) was delivered using subcutaneously implanted Alzet micro-osmotic pumps (Model 1002, Durchet Corporation, Cupertino, CA). Alzet pumps delivered a constant dose of rh-Rlx at 0.35 μg/hr. Alzet pumps were implanted in hind leg tumor model when tumors reached 5 mm in diameter and in the DSC tumor model when tumors reached 2 mm in diameter. Expression and mobility studies were performed 3 days following osmotic pump implantation.

### Treatment Groups

Tumors were divided into four treatment groups. The control group (R−EP−) consisted of tumors in untreated mice without exposure to external electric fields. The rh-Rlx treatment group (R+EP−) consisted of tumors in rh-Rlx treated mice without exposure to external electric fields. The electric field treatment group (R−EP+) consisted of tumors in untreated mice that exposed to external electric fields. The rh-Rlx with electric field treatment group (R+EP+) consisted of tumors in rh-Rlx treated mice that exposed to external electric fields.

### Hydroxyproline Assay

A hydroxyproline assay was performed to determine the average collagen content of 4T1 and B16.F10 tumors in hind leg and DSC models. Tumors were excised from animals and incubated in 1.0 ml digesting buffer (126 μg/ml papain in 0.1 M $NaHPO_4$, 5.0 mM EDTA, and 5.0 mM L-cysteine-HCL, pH 6.0) for 20 h at 60°C. 100 μl of each papain digest were then hydrolysed in 900 μl 6 N HCl for 20 h at 115°C.

Samples were brought to room temperature and two drops of 0.02% methyl red indicator were added. Sample solutions were neutralized with 2.5 M NaOH, followed by 0.5 M HCl and, finally, 0.5 M NaOH. The final volume, following titration, of each sample was determined. 0.5 ml chloramine T solution (705 mg chloramine T in 40 ml pH 6.0 buffer and 5 ml isopropanol) was then added to 1.0 ml of each sample and allowed to stand for 20 min at room temperature. The pH 6.0 buffer consisted of 5.0 g citric acid monohydrate, 12.0 g sodium acetate trihydrate, 3.4 g NaOH, and 1.2 ml glacial acetic acid brought to 100 ml with distilled water. 0.5 ml pDAB solution (4.0 g p-dimethylaminobenzaldehyde (pDAB) in 16.0 ml isopropanol and 7.0 ml perchloric acid (60%)) was added and samples were incubated for 20 min at 60°C. Samples were cooled in a water bath at the room temperature for 5 min.

The absorbance of the solutions at 557 nm was recorded within 1 h following cooling. A standard hydroxyproline curve was established by dissolving 0–5 μg hydroxyproline in 1 ml deionized water and repeating the above procedure from the addition of chloramine T. Hydroxyproline, an amino acid derivative exclusive to collagen, accounts for approximately 12.5 % of the total collagen mass (19).

### pDNA Electromobility Studies

On day 3 following Alzet pump implantation (tumors reached 3–4 mm in diameter), mice bearing DSC tumors were anesthetized and approximately 1 μg of rhodamine-labeled plasmid DNA (Rho-pDNA, 5.1 kb, Gene Therapy Systems, San Diego, CA) was injected into the center of the tumor using a microinjection system consisting of a TransferMan NK micromanipulator and a CellTram Vario oil pump (Eppendorf, Westbury, NY) mounteds on an Axioskop 2 Plus upright microscope (Zeiss, Thornwood, NY). This method allowed precise control over the location and amount of pDNA delivered while limiting damages to tumor tissue and vasculature. The tissue was washed thoroughly with PBS, and the DSC was resealed with a sterile glass coverslip.

Anesthetized mice were secured on a custom designed stage for a confocal microscope (Model 510, Zeiss). A localized electric field was applied using two stainless steel, parallel plate electrodes on the skin side of the DSC (2). An electric potential difference was supplied by an ECM 830 electro square porator (BTX). Pulsed electric fields examined in this study consisted of 10 identical square voltage pulses with a magnitude of 100 or 400 V/cm and a duration of 20 or 50 ms. The interval between consecutive pulses was 1 s.

Fluorescence images of the Rho-pDNA and YG-MS were acquired using a 40X objective before and immediately following the application of an entire 10-pulse sequence. The area of

the image was away from the needle track to ensure the tissue imaged was not damaged during plasmid administration. The one-dimensional resolution of the acquired images was 0.44 μm/pixel. A cross-correlation analysis was performed on the fluorescence images taken before and following application of the pulsed electric field. Analysis was performed independently on channel 1 and channel 2 to determine the displacement vectors, averaged over a field of view, of the Rho-pDNA ($\vec{D}_{\mathrm{pDNA}}$) and YG-MS ($\vec{D}_{\mathrm{MS}}$), respectively. Details of the cross-correlation analysis are provided elsewhere (19).

Due to their size and neutral charge, YG-MSs were assumed to have been locked in place with respect to surrounding tissues and were therefore used as markers for tissue movement. The electric field-induced pDNA movement, defined as the pDNA displacement relative to the tumor tissue, was determined on a per pulse basis by,

$$d_p = \frac{|\vec{D}_{\mathrm{pDNA}} - \vec{D}_{\mathrm{MS}}|}{N} \quad (1)$$

where $d_p$ is the electric field-induced pDNA movement per pulse and $N$ is the number pulses in the applied field, which was equal to 10 in this study.

## Transgene Expression Studies

Non-invasive bioluminescence imaging was used to indirectly quantify gene transport in the hind leg tumor models. Direct electromobility measurements could not be made in the hind leg tumors due to the inaccessibility of these models with confocal microscopy. On day 3 following Alzet pump implantation, pCMVLuc was administered into the tumor. A 30-gauge needle was inserted into the center of the tumor and 5 μg of pCMVLuc in 50 μl PBS was infused at 1 μl/s using a PHD 2000 infusion pump (Harvard Apparatus, Holliston, MA).

For the R−EP+ and R+EP+ tumor groups, 10 s following pCMVLuc administration, a pulsed electric field was applied across the tumor using caliper electrodes. The electric field consisted of 10 pulses with 400 V/cm in strength, 20 ms in duration, and 1 s interval between pulses. The power supply used was an ECM 830 electro square porator (BTX, San Diego, CA).

Twenty-four hours following electric field application, transgene expression was quantified using a Xenogen *In vivo* Imaging System (IVIS, Xenogen, Alameda, CA). Mice were anesthetized in an induction chamber with 2% Isoflurane and maintained under anesthesia throughout the course of luciferase measurement. Mice were given an i.p. injection of 50 μl aqueous D-luciferin solution (28.6 mg/ml). Twenty minutes later, mice were placed in the Xenogen IVIS and a grey scale reference image was acquired under low-level illumination. Then, a bioluminescence image was acquired by integrating photons emitted from the animals over a 30-second period. The two images were overlaid, and the luciferase expression was displayed as the number of photons emitted per second per square centimeter per steridian (sr). Luciferase expression in the tumor was later quantified as the sum of the total photon flux over the surface of the tumor using the Living Image Software (Xenogen).

## Collagen Binding Assay

To explore the potential mechanisms behind the correlation between collagen content and pDNA electromobility, a collagen binding assay was performed in which agarose (Sigma, St. Louis, MO) or Type I collagen (from rat tail, BD™, Franklin Lakes, NJ) gel was formed in 35 mm petri dishes at 0.1 % w/v and the volume of gel was 3.0 ml. Gels of this concentration were used to reduce the steric hindrance to transport through the fiber matrix, and therefore accentuate the hindrance caused by electrostatic interactions between agarose or collagen fiber and pDNA, which was expected in the collagen gel but not the agarose gel. Approximately

0.01 μl of pDNA solution containing either Rho-pDNA at 0.05 μg/ml, or a mixture of Rho-pDNA at 0.05 μg/ml and unlabeled pDNA at 0.45 μg/ml were microinjected into the center of the gel. Fluorescence images of the Rho-pDNA were acquired, using a 10X objective on an inverted microscope (Axiovert 100 TV, Zeiss), and captured with an intensified CCD camera (DAGE-MTI, Inc., Michigan City, IN). Images were taken at t = 0, 1, 2, and 3 h, where t = 0 represented the time 10 s following pDNA injection. At this time, injection-driven convection had concluded, and diffusion represented the only acting transport mechanism. The average diameters of distribution volume of Rho-pDNA in different gels were measured with an image analysis software (Image-Pro Plus®, Media Cybernetics, Inc., Silver Spring, MD), and normalized by their values at t = 0. The experiment was repeated three times.

### Statistical analysis

Statistically significant differences in the mean net pDNA movement per pulse and mean photon flux were tested with a Mann-Whitney test. All statistical calculations were performed using Minitab statistical software (Minitab Inc, State College, PA).

## RESULTS

### Tumor Collagen Content

The collagen contents in 4T1 and B16.F10 tumors grown either in the DSC or the hind leg in rh-Rlx treated mice were quantified and compared with previously determined values in the same mouse tumor models without rh-Rlx treatment (see Table 1). For DSC tumors, the rh-Rlx treatment increased the collagen contents in all 4T1 tumors, with the minimum concentration in the treated group being 42% higher than the maximum value in the control group. However, the response of B16.F10 tumors to the rh-Rlx treatment was inconsistent in three repeated experiments. For hind leg tumors, the rh-Rlx treatment significantly decreased collagen concentrations in all tumors, with the maximum concentrations in the treated group being reduced to 58% and 31% of the minimum values in the control group, in 4T1 and B16.F10 tumors, respectively. These results suggested that tissue microenvironment played an important role in tumor responses to relaxin treatment.

### Interstitial Electromobility of Plasmid DNA in DSC Tumor Model

pDNA electromobility in the interstitial space was quantified directly in the DSC tumors treated chronically with rh-Rlx. Four different electric fields were used in the study, consisting of 10 square wave pulses with 100 or 400 V/cm in field strength, 20 or 50 ms in duration, and 1 s interval between pulses. The distances of transport are shown in Figure 1 for both 4T1 and B16.F10 tumors (R+); and they were compared with those observed in a previous study without rh-Rlx treatment (R−) (2). The comparison showed that rh-Rlx treatment did not result in a significant increase in electromobility for all four electric fields examined ($P > 0.05$).

### Transgene Expression in Hind Leg Tumor Model

Interstitial transport in hind leg tumors, where rh-Rlx treatment resulted in a significant decrease in the collagen content, was examined indirectly via the enhancement of reporter gene expression. The *in vivo* expression was monitored in hind leg tumors grown in untreated mice (R−) and rh-Rlx treated mice (R+), either without exposure to external electric field (EP−) or at 24 hours following the exposure to external field (EP+). In this experiment, only one type of electric field was applied to tumors. It consisted of 10 pulses with 400 V/cm in field strength, 20 ms in duration, and 1 s interval between pulses.

A representative transgene expression image is shown in Figure 2A. The total transgene expression within a tumor was quantified as the photon flux, and the mean photon fluxes from

both tumors in each treatment group are shown in Figure 2B. Exposure to external electric field significantly increased transgene expression in both 4T1 and B16.F10 tumors ($P < 0.01$); and the results were independent of rh-Rlx treatment. In tumors exposed to external electric field, rh-Rlx treatment could further enhance transgene expression in 4T1 tumor ($P = 0.04$), but not in B16.F10 tumor ($P = 0.25$). Rh-Rlx treatment alone had no effects on transgene expression in either 4T1 or B16.F10 tumors.

### pDNA Binding to Collagen

To investigate potential mechanisms behind the correlation between pDNA transport and tumor collagen content, an *in vitro* assay was performed to compare the diffusivity of pDNA in agarose and collagen gels. It was observed that Rho-pDNA could diffuse freely through the agarose gel but its diffusion in the collagen gel exhibited characteristics of pDNA binding with collagen fibers, as indicated by changes in the normalized diameter of pDNA distribution volume ($D_N$) (see Figure 3). $D_N$ reached a plateau within 1 h following Rho-pDNA injection into the collagen gel. The distribution volume of Rho-pDNA in the collagen gel could be increased significantly when it was mixed with unlabeled pDNA at a ratio of 9:1 (w/w) in the solution before injecting into the collagen gel, indicating a competitive binding between the labeled and unlabeled pDNA with specific binding sites on collagen fibers. In order to compare the data of $D_N$ from different experiments, in which the initial radius of distribution volume, a, might differ, the time of diffusion was normalized by $a^2$. Therefore, the curves shown in Figure 3 were independent of the initial radius.

## DISCUSSION

The role of electrophoresis played in electric field-mediated gene delivery *in vivo* remains a subject of considerable debate. Some studies suggest that electrophoresis plays a critical role in gene transfer following electropermeabilization (18), and others suggest that electrophoresis is not even involved (36). Adding to this ambiguity, few studies have distinguished between electrophoresis through porous matrix compartments (*e.g.*, interstitium and cytosol) and across membrane barriers (*e.g.*, cell membrane and nuclear envelope). In a recent study, the magnitude of *in vivo* electrophoresis in tumor interstitium was quantified directly for the first time (2). High-energy electrophoretic pulses (400 V/cm, 50 ms) were able to induce interstitial transport but the total distance after application of 10 pulses was less than 2.5 μm, or approximately one fourth the diameter of a typical tumor cell, in either 4T1 or B16.F10 tumor. The short distance could be caused by collagen fibers since previous studies have demonstrated that collagen matrix is the major barrier to interstitial macromolecular transport (19,24,25,37). Therefore, alterations in the collagen component of tumor ECM may improve electric field-induced interstitial pDNA transport, thereby improving efficiency of pDNA delivery. To investigate this possibility, effects of rh-Rlx on tumor collagen contents were measured in this study. It was observed that the collagen contents were reduced in 4T1 and B16.F10 tumors grown in the hind leg of rh-Rlx treated mice. However, the collagen contents of 4T1 and B16.F10 tumors were increased in most tumors transplanted in DSCs (see Table 1). This finding was consistent with another report published in the literature, in which rh-Rlx treatment did not reduce the overall collagen levels in DSC tumor models (34). The dependency of rh-Rlx-induced changes in collagen content on tumor type and location of tumor transplantation may be attributed to the following mechanisms.

Firstly, the developmental stage of the tumors varied between the hind leg and DSC tumor models. Both tumor models were seeded by a subcutaneous injection of tumor cell suspensions. However, the hind leg tumors were ~5 mm in diameter whereas the DSC tumors were only ~2 mm in diameter at the initiation of rh-Rlx treatment. This difference in initial tumor age and size might have translated into the difference in intrinsic rates of collagen metabolism between

the two tumor models, and therefore different tumor responses to rh-Rlx treatment. Secondly, the intrinsic level of collagen in 4T1 tumors grown on the hind leg was much higher than that in the DSC although there was < 2-fold difference in the collagen contents for B16.F10 tumors grown at different places (see Table 1). This discrepancy could be caused by various factors in tissue microenvironment, which are dependent on tumor type and site of transplantation (25,38). This is because tumor ECM is largely produced by host stromal cells (38,39). Due to their different anatomical locations, DSC and hind leg tumors may have developed different ECM. Thirdly, the anatomical location of the allograft may have influenced the extent of tumor vascularization. While the systemic rh-Rlx dosage was equal for both tumor models, the local concentration of rh-Rlx depended on tumor vasculature. Hind leg tumors were implanted on the highly vascularized quadricep muscle, and therefore might have had the opportunity to recruit significantly more neovascularization during the course of the study than DSC tumors, which were established in a less vascularized DSC environment. A highly vascularized hind leg tumor would have received a greater rh-Rlx dose than the less vascularized DSC tumor, which might have accounted for the greater effect of rh-Rlx treatment on the collagen content of the hind leg tumors. Finally, the net change in the collagen content depend on the interplay between collagen synthesis and collagen degradation (27,34). Both can be upregulated by relaxin. As a result, the relaxin treatment might have reduced the collagen fiber length but not necessarily the total content (see Table 1) (34).

The collagen contents in tumors were correlated with the efficiency of gene transfer. In the hind leg tumors, where the collagen content was reduced significantly, rh-Rlx treatment increased the mean transgene expression in both 4T1 and B16.F10 tumors (see Figure 2B). The collagen content, and the content reduction, were greater in 4T1 tumors that in B16.F10 tumors, which might attribute to the level of significance in the improvement of transgene expression since the improvement was statistically significant only in 4T1 tumors. It was likely that the extent of improvement in B16.F10 tumors was less than inter-tumoral data variation, caused presumably by tumor heterogeneity (see Figure 2B), so that the improvement was statistically insignificant. In light of the dependence of gene transfer on pDNA interstitial transport, which in turn depended on tissue collagen content, it was likely that the increased transgene expression in rh-Rlx treated hind leg tumors was the result of improved electromobility of pDNA. Relaxin treatment alone, without electric field treatment, did not result in any increase in transgene expression, indicating that rh-Rlx treatment did not directly influence gene transfer.

Without exposure to external electric fields, transgene expression was significantly greater in 4T1 tumors than B16.F10 tumors, in both untreated and rh-Rlx treated mice ($P < 0.05$). This difference might be attributed partly to endocytosis or macropinocytosis of pDNA by various cells in these tumors since they were the only possible mechanisms known for gene transfer via naked pDNA (36,40,41). The amount of endocytosed or macropinocytosed pDNA depends on the number of cells that are close to pDNA infused into tumors. Therefore, parameters for intratumoral infusion of pDNA might play an important role in determining the transgene expressions shown in Figure 2 (42–45). The infusion conditions used in this study had previously been optimized for maximizing the spatial distribution of gene vectors in 4T1 hind leg tumors (46). As a result, it was likely that pDNA was available to more cells in 4T1 tumors than in B16.F10 tumors. Following the exposure to external electric field, the difference in transgene expression between the two tumors was no longer significant ($P > 0.05$), showing the electric field to be effective in reducing some heterogeneity observed across tumor types.

In the DSC tumor model, where the collagen content was slightly increased, rh-Rlx treatment did not increase the electromobility of pDNA for any of the four electric fields investigated (see Figure 1). This observation was consistent with previous studies correlating interstitial pDNA electromobility with the collagen content (19), but differed from that in another study

where rh-Rlx treatment enhanced diffusion of IgG and dextran-2M in DSC tumors (34). The enhancement was attributed to the reduction in collagen fiber length instead of total collagen content, which loosened fiber matrix structures and increased pore size in extracellular matrix. As a result, the resistance to diffusion of macromolecules was reduced (34). In this study, it was possible that the pore size was not adequately increased for pDNA transport after relaxin treatment since pDNA is larger than IgG and dextran. More importantly, pDNA is a highly negatively charged molecule and its transport can be significantly hindered by charge-charge interactions with collagen fibers. These interactions were likely to be a main mechanism for explaining the lack of improvement in pDNA electromobility in relaxin treated tumors grown in DSC.

To mimic the charge-charge interactions, passive transport of pDNA in collagen gel was investigated and compared to that in agarose gel. In agarose gel, where only steric interactions between Rho-pDNA and agarose fibers were expected, Rho-pDNA transport followed the expected pattern of free diffusion through a porous matrix. However, Rho-pDNA diffusion through the collagen gel indicated that binding of Rho-pDNA to collagen had occurred because the diameter of Rho-pDNA distribution volume quickly reached a plateau after injection into the gel (see Figure 3). When unlabeled pDNA was added, Rho-pDNA was able to diffuse a greater distance from the site of injection. This behavior was characteristic of the unlabeled pDNA competing with the Rho-pDNA for available binding sites on collagen fibers. By blocking these binding sites, the unlabeled pDNA allowed the Rho-pDNA to distribute to a greater volume around the injection site. pDNA-collagen binding has been suggested previously in studies when investigating the use of implantable pDNA-embedded collagen matrices for sustained release (47). Cohen-Sacks *et al.* showed that 60–80% of embedded pDNA was released from the collagen matrix within 2 h when submerged in TE buffer. The remaining pDNA was not released from the collagen gel until SDS detergent was added to the buffer. The authors proposed that SDS was required to break an electrostatic interaction between pDNA and the free lysine groups in the collagen (47). Binding of pDNA to collagen fibers might explain the apparent discrepancy between the findings reported here, and those reported previously by Brown *et al.* (34), because IgG and dextran-2M could not bind to collagen strongly. The binding phenomenon might also explain why rh-Rlx treatment resulted in no increase in pDNA mobility in 4T1 tumors in the DSC model (see Figure 1) but an enhancement in transgene expression in the hind leg model (see Figure 2), suggesting that it would be the collagen content, regardless of its matrix structures, that determined the hindrance to pDNA transport.

In summary, results from this study demonstrated that effects of rh-Rlx on the collagen content depended on microenvironment in tumor tissues and that rh-Rlx treatment would enhance electric field-mediated gene delivery only if it could effectively reduce the collagen content in collagen-rich tumors. The results also suggested that the mechanism of enhancement was due to improvement in interstitial transport of pDNA. In future studies, the correlation between increased gene transfer and improved interstitial transport needs to be verified directly in certain DSC tumor models in which the collagen content can be significantly reduced by either infecting tumors with adenoviral vector for relaxin (35) or co-injecting collagenase with pDNA into tumors (48).

## ACKNOWLEGMENTS

This work was supported in part by a grant from the National Institutes of Health (CA94019). The recombinant human relaxin used in this study was generously supplied by BAS Medical (San Mateo, CA).

## REFERENCES


1. Heller LC, Heller R. In vivo electroporation for gene therapy. Hum Gene Ther 2006;17:890–897. [PubMed: 16972757]
2. Henshaw JW, Zaharoff DA, Mossop BJ, Yuan F. Electric field-mediated transport of plasmid DNA in tumor interstitium in vivo. Bioelectrochemistry 2007;71:233–242. [PubMed: 17728192]
3. Henshaw JW, Yuan F. Field distribution and DNA transport in solid tumors during electric field-mediated gene delivery. J Pharm Sci 2008;97:691–711. [PubMed: 17624918]
4. Neumann E. Membrane electroporation and direct gene transfer. Bioelectrochem Bioenerg 1992;28:247–267.
5. Wolf H, Rols MP, Boldt E, Neumann E, Teissie J. Control by pulse parameters of electric field-mediated gene transfer in mammalian cells. Biophys J 1994;66:524–531. [PubMed: 8161705]
6. Bae C, Butler PJ. Automated single-cell electroporation. Biotechniques 2006;41:399–402. [PubMed: 17068953]
7. Mir LM, Bureau MF, Gehl J, Rangara R, Rouy D, Caillaud JM, et al. High-efficiency gene transfer into skeletal muscle mediated by electric pulses. Proc Natl Acad Sci U S A 1999;96:4262–4267. [PubMed: 10200250]
8. Heller L, Jaroszeski MJ, Coppola D, Pottinger C, Gilbert R, Heller R. Electrically mediated plasmid DNA delivery to hepatocellular carcinomas in vivo. Gene Ther 2000;7:826–829. [PubMed: 10845719]
9. Wells JM, Li LH, Sen A, Jahreis GP, Hui SW. Electroporation-enhanced gene delivery in mammary tumors. Gene Ther 2000;7:541–547. [PubMed: 10819568]
10. Lohr F, Lo DY, Zaharoff DA, Hu K, Zhang X, Li Y, et al. Effective tumor therapy with plasmid-encoded cytokines combined with in vivo electroporation. Cancer Res 2001;61:3281–3284. [PubMed: 11309280]
11. Lucas ML, Heller L, Coppola D, Heller R. IL-12 plasmid delivery by in vivo electroporation for the successful treatment of established subcutaneous B16.F10 melanoma. Mol Ther 2002;5:668–675. [PubMed: 12027550]
12. Li S, Ma Z. Nonviral gene therapy. Curr Gene Ther 2001;1:201–226. [PubMed: 12108955]
13. Mir LM, Moller PH, Andre F, Gehl J. Electric pulse-mediated gene delivery to various animal tissues. Adv Genet 2005;54:83–114. [PubMed: 16096009]
14. Heller LC, Ugen K, Heller R. Electroporation for targeted gene transfer. Expert Opin Drug Deliv 2005;2:255–268. [PubMed: 16296752]
15. Cemazar M, Golzio M, Sersa G, Rols MP, Teissie J. Electrically-assisted nucleic acids delivery to tissues in vivo: where do we stand? Curr Pharm Des 2006;12:3817–3825. [PubMed: 17073680]
16. Prud'homme GJ, Glinka Y, Khan AS, Draghia-Akli R. Electroporation-enhanced nonviral gene transfer for the prevention or treatment of immunological, endocrine and neoplastic diseases. Curr Gene Ther 2006;6:243–273. [PubMed: 16611045]
17. Bureau MF, Gehl J, Deleuze V, Mir LM, Scherman D. Importance of association between permeabilization and electrophoretic forces for intramuscular DNA electrotransfer. Biochim Biophys Acta 2000;1474:353–359. [PubMed: 10779687]
18. Satkauskas S, Andre F, Bureau MF, Scherman D, Miklavcic D, Mir LM. Electrophoretic component of electric pulses determines the efficacy of in vivo DNA electrotransfer. Hum Gene Ther 2005;16:1194–1201. [PubMed: 16218780]
19. Zaharoff DA, Barr RC, Li CY, Yuan F. Electromobility of plasmid DNA in tumor tissues during electric field-mediated gene delivery. Gene Ther 2002;9:1286–1290. [PubMed: 12224011]
20. Ogston AG, Sherman TF. Effects of hyaluronic acid upon diffusion of solutes and flow of solvent. J Physiol 1961;156:67–74. [PubMed: 13730461]
21. Winlove, CP.; Parker, KH. The physiological function of the extracellular matrix. In: Reed, RK.; Laine, GA.; Bert, JL.; Winlove, CP., editors. Interstitiu, Connective Tissue and Lymphatics. London: Portland Press; 1987. p. 137-165.
22. Liotta LA, Rao CN. Role of the extracellular matrix in cancer. Ann N Y Acad Sci 1985;460:333–344. [PubMed: 3008626]

23. Ronnov-Jessen L, Petersen OW, Bissell MJ. Cellular changes involved in conversion of normal to malignant breast: importance of the stromal reaction. Physiol Rev 1996;76:69–125. [PubMed: 8592733]
24. Netti PA, Berk DA, Swartz MA, Grodzinsky AJ, Jain RK. Role of extracellular matrix assembly in interstitial transport in solid tumors. Cancer Res 2000;60:2497–2503. [PubMed: 10811131]
25. Pluen A, Boucher Y, Ramanujan S, McKee TD, Gohongi T, di Tomaso E, et al. Role of tumor-host interactions in interstitial diffusion of macromolecules: cranial vs. subcutaneous tumors. Proc Natl Acad Sci U S A 2001;98:4628–4633. [PubMed: 11274375]
26. Ramanujan S, Pluen A, McKee TD, Brown EB, Boucher Y, Jain RK. Diffusion and convection in collagen gels: implications for transport in the tumor interstitium. Biophys J 2002;83:1650–1660. [PubMed: 12202388]
27. Bani D. Relaxin: a pleiotropic hormone. Gen Pharmacol 1997;28:13–22. [PubMed: 9112071]
28. Vasilenko P, Mead JP. Growth-promoting effects of relaxin and related compositional changes in the uterus, cervix, and vagina of the rat. Endocrinology 1987;120:1370–1376. [PubMed: 3830054]
29. Bani G, Maurizi M, Bigazzi M, Bani Sacchi T. Effects of relaxin on the endometrial stroma. Studies in mice. Biol Reprod 1995;53:253–262. [PubMed: 7492676]
30. Garber SL, Mirochnik Y, Brecklin CS, Unemori EN, Singh AK, Slobodskoy L, et al. Relaxin decreases renal interstitial fibrosis and slows progression of renal disease. Kidney Int 2001;59:876–882. [PubMed: 11231342]
31. Unemori EN, Pickford LB, Salles AL, Piercy CE, Grove BH, Erikson ME, et al. Relaxin induces an extracellular matrix-degrading phenotype in human lung fibroblasts in vitro and inhibits lung fibrosis in a murine model in vivo. J Clin Invest 1996;98:2739–2745. [PubMed: 8981919]
32. Wiqvist I, Norstrom A, O'Byrne E, Wiqvist N. Regulatory influence of relaxin on human cervical and uterine connective tissue. Acta Endocrinol (Copenh) 1984;106:127–132. [PubMed: 6587712]
33. Unemori EN, Amento EP. Relaxin modulates synthesis and secretion of procollagenase and collagen by human dermal fibroblasts. J Biol Chem 1990;265:10681–10685. [PubMed: 2162358]
34. Brown E, McKee T, diTomaso E, Pluen A, Seed B, Boucher Y, et al. Dynamic imaging of collagen and its modulation in tumors in vivo using second-harmonic generation. Nat Med 2003;9:796–800. [PubMed: 12754503]
35. Kim JH, Lee YS, Kim H, Huang JH, Yoon AR, Yun CO. Relaxin expression from tumor-targeting adenoviruses and its intratumoral spread, apoptosis induction, and efficacy. J Natl Cancer Inst 2006;98:1482–1493. [PubMed: 17047197]
36. Liu F, Heston S, Shollenberger LM, Sun B, Mickle M, Lovell M, et al. Mechanism of in vivo DNA transport into cells by electroporation: electrophoresis across the plasma membrane may not be involved. J Gene Med 2006;8:353–361. [PubMed: 16353289]
37. Choi J, Credit K, Henderson K, Deverkadra R, He Z, Wiig H, et al. Intraperitoneal immunotherapy for metastatic ovarian carcinoma: Resistance of intratumoral collagen to antibody penetration. Clin Cancer Res 2006;12:1906–1912. [PubMed: 16551876]
38. Fukumura D, Xavier R, Sugiura T, Chen Y, Park EC, Lu N, et al. Tumor induction of VEGF promoter activity in stromal cells. Cell 1998;94:715–725. [PubMed: 9753319]
39. Brown LF, Guidi AJ, Schnitt SJ, Van De Water L, Iruela-Arispe ML, Yeo TK, et al. Vascular stroma formation in carcinoma in situ, invasive carcinoma, and metastatic carcinoma of the breast. Clin Cancer Res 1999;5:1041–1056. [PubMed: 10353737]
40. Rols MP, Femenia P, Teissie J. Long-lived macropinocytosis takes place in electropermeabilized mammalian cells. Biochem Biophys Res Commun 1995;208:26–35. [PubMed: 7887937]
41. Antov Y, Barbul A, Mantsur H, Korenstein R. Electroendocytosis: exposure of cells to pulsed low electric fields enhances adsorption and uptake of macromolecules. Biophys J 2005;88:2206–2223. [PubMed: 15556977]
42. McGuire S, Zaharoff D, Yuan F. Nonlinear dependence of hydraulic conductivity on tissue deformation during intratumoral infusion. Ann Biomed Eng 2006;34:1173–1181. [PubMed: 16791492]
43. McGuire S, Yuan F. Quantitative analysis of intratumoral infusion of color molecules. Am J Physiol Heart Circ Physiol 2001;281:H715–H721. [PubMed: 11454575]

44. Zhang XY, Luck J, Dewhirst MW, Yuan F. Interstitial hydraulic conductivity in a fibrosarcoma. Am J Physiol Heart Circ Physiol 2000;279:H2726–H2734. [PubMed: 11087227]

45. Wang Y, Yuan F. Delivery of viral vectors to tumor cells: extracellular transport, systemic distribution, and strategies for improvement. Ann Biomed Eng 2006;34:114–127. [PubMed: 16520902]

46. Wang Y, Yang Z, Liu S, Kon T, Krol A, Li CY, et al. Characterisation of systemic dissemination of nonreplicating adenoviral vectors from tumours in local gene delivery. Br J Cancer 2005;92:1414–1420. [PubMed: 15812558]

47. Cohen-Sacks H, Elazar V, Gao J, Golomb A, Adwan H, Korchov N, et al. Delivery and expression of pDNA embedded in collagen matrices. J Control Release 2004;95:309–320. [PubMed: 14980779]

48. McKee TD, Grandi P, Mok W, Alexandrakis G, Insin N, Zimmer JP, et al. Degradation of fibrillar collagen in a human melanoma xenograft improves the efficacy of an oncolytic herpes simplex virus vector. Cance Res 2006;66:2509–2513.

## Abbreviations

pDNA, plasmid DNA; DSC, dorsal skin-fold chamber; rh-Rlx, recombinant human relaxin; ECM, extracellular matrix; GAG, glycosaminoglycan.

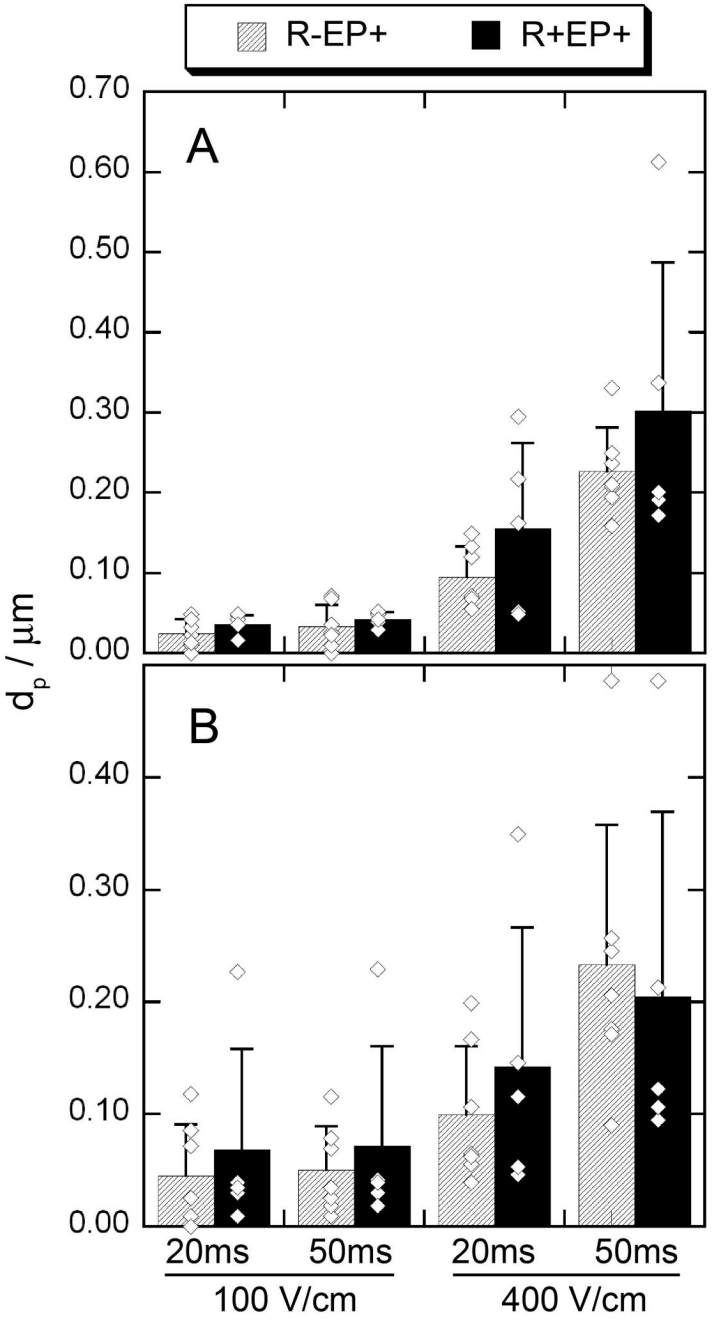


**Figure 1.**

Net distance of pDNA movement per pulse in untreated (black) and rh-Rlx treated (grey) 4T1 (A) and B16.F10 (B) tumors grown in DSCs. The applied electric field consisted of 10 square wave pulses with 100 or 400 V/cm in strength, 20 or 50 ms in duration, and 1 s interval between pulses. The symbols represent individual data points and the error bars represent the standard deviation from the mean (n = 7 for untreated and n = 5 for rh-Rlx treated tumors).

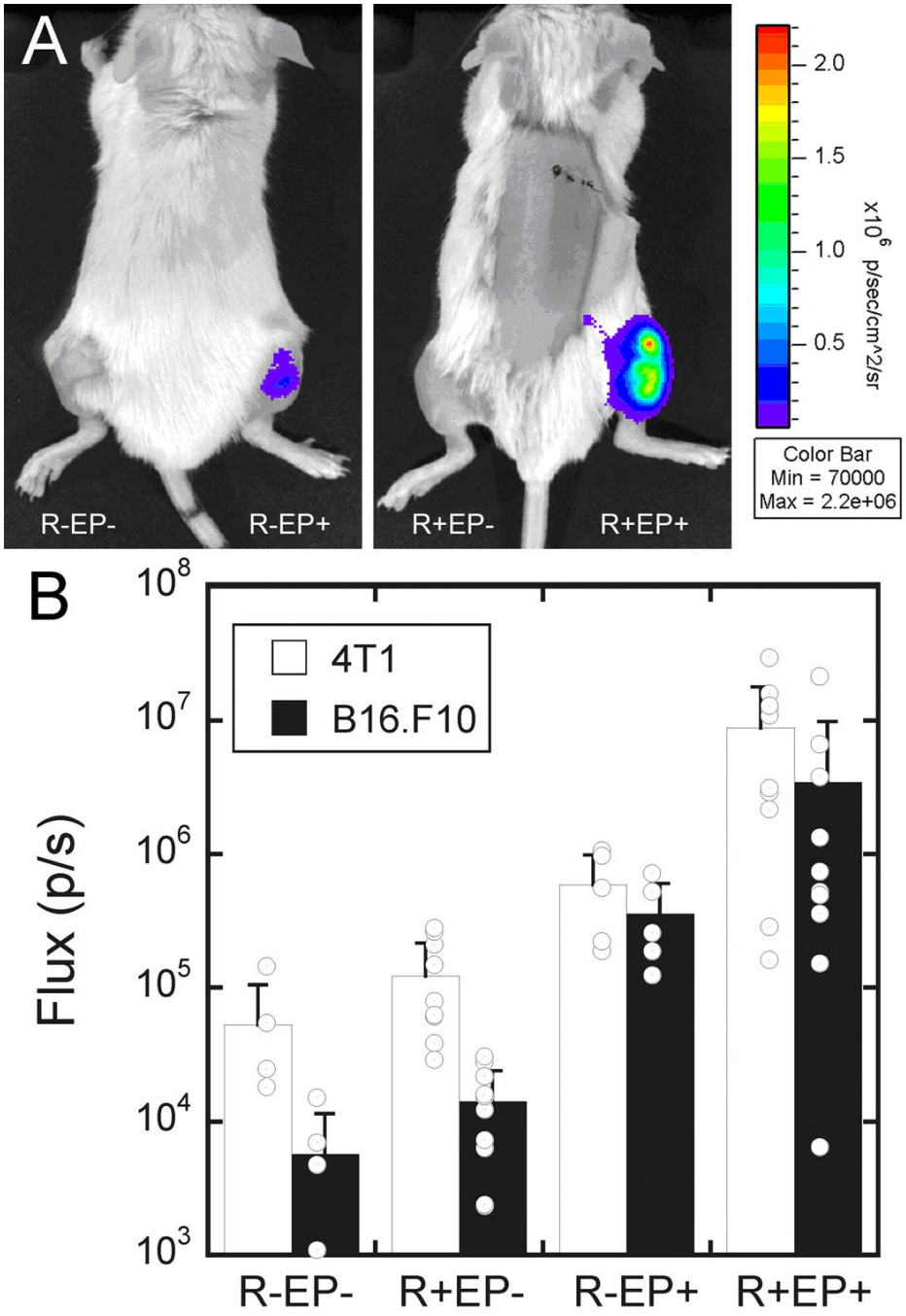


**Figure 2.**

(A) Representative images of bioluminescence in 4T1 tumors grown in the hind leg in different groups and (B) amount of transgene expression in 4T1 and B16.F10 tumors grown the hind leg in each treatment group. The treatment groups are as follows: R−EP−, tumors receiving pDNA infusion; R+EP−, tumors receiving pDNA infusion and rh-Rlx treatment; R−EP+, tumors receiving pDNA infusion and electric treatment; and R+EP+, tumors receiving pDNA infusion, rh-Rlx treatment, and electric treatment. The symbols represent individual data points. The bars show the mean proton fluxes over the entire surface of tumors; and the error bars represent the standard deviation from the mean (n = 5 in R−EP− and R−EP+ groups; n = 10 in R+EP− and R+EP+ groups).

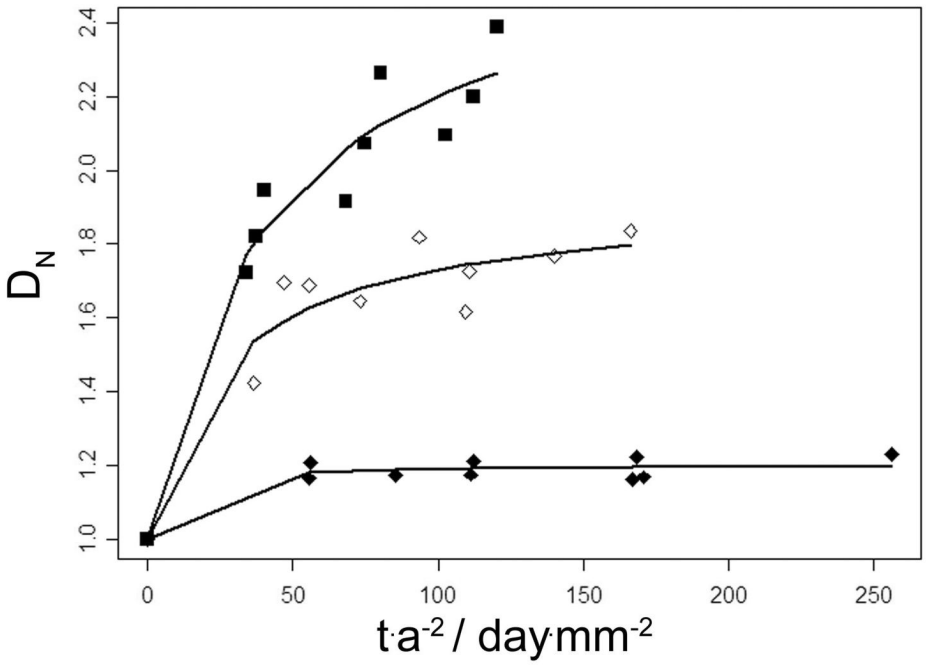


**Figure 3.**

Diameter of pDNA distribution volume normalized by its value at t = 0 ($D_N$). The diameter was quantified at different time points following the injection of pDNA solutions into collagen (diamonds) or agarose (squares) gel. The time was normalized by $a^2$, which is the square of the initial radius of distribution volume. The injected solution contained either Rho-pDNA at 0.05 μg/ml (filled symbols) or a mixture of Rho-pDNA at 0.05 μg/ml and unlabelled pDNA at 0.45 μg/ml (open symbols).

**TABLE 1**

Tumor collagen content in control and rh-Rlx treated tumors

| | Hind Leg | | | | Dorsal Skin-Fold Chamber | | | |
|---|---|---|---|---|---|---|---|---|
| | 4T1 | | B16.F10 | | 4T1 | | B16.F10 | |
| | Con[&] | rh-Rlx | Con | rh-Rlx | Con | rh-Rlx | Con | rh-Rlx |
| T1 | 14.73[*] | 8.48 | 2.45 | 0.75 | 4.63 | 7.06 | 3.44 | 5.66 |
| T2 | 19.40 | 7.87 | 2.50 | 0.56 | 4.32 | 9.61 | 3.35 | 6.74 |
| T3 | 27.19 | 4.23 | 2.62 | 0.74 | 4.98 | 14.17 | 5.98 | 3.13 |
| *Avg* | *20.44* | *6.88* | *2.52* | *0.68* | *4.64* | *10.28* | *4.26* | *5.17* |

[&]Con = untreated tumor; Ti = tumor number for i = 1, 2, 3; Avg = average values of three tumors.

[*]Units of all values are μg collagen per mg wet tissue.